PROTEINS: Structure, Function, and Genetics 21:237–243 (1995)

Dramatic Differences in the Motions of the Mouth of Open and Closed Cytochrome P450BM-3 by Molecular Dynamics Simulations

Mark D. Paulsen and Rick L. Ornstein
Environmental Molecular Sciences Laboratory, Pacific Northwest Laboratory, Richland, Washington, 99352

ABSTRACT **Molecular dynamics trajectories were calculated separately for each of the two molecules in the asymmetric unit of the crystal structure of the hemoprotein domain of cytochrome P450BM-3. Each simulation was 200 ps in length and included a 10 Å layer of explicit solvent. The simulated time-average structure of each P450BM-3 molecule is closer to its crystal structure than the two molecular dynamics time-averaged structures are to each other. In the crystal structure, molecule 2 has a more accessible substrate binding pocket than molecule 1, and this difference is maintained throughout the simulations presented here. In particular, the substrate docking regions of molecule 1 and molecule 2 diverge in the solution state simulations. The mouth of the substrate binding pocket is significantly more mobile in the simulation of molecule 2 than in the simulation of molecule 1. For molecule 1, the width of the mouth is only slightly larger than its X-ray value of 8.7 Å and undergoes fluctuations of about 1 Å. However, in molecule 2, the mouth of the substrate binding pocket is dramatically more open in the time-average molecular dynamics structure (14.7 Å) than in the X-ray structure (10.9 Å). Furthermore, this region of the protein undergoes large amplitude motions during the trajectory that are not seen in the trajectory of molecule 1, repeatedly opening and closing up to 7 Å. Presumably, the binding of different substrates will induce the mouth region to adopt different conformations from within the wide range of structures that are accessible.** © 1995 Wiley-Liss, Inc.*

Key words: domain motions, crystal packing effects, protein dynamics, induced-fit, enzyme dynamics

INTRODUCTION

While for some proteins, such as cytochrome P450cam, substrates and inhibitors bind to what appears to be an essentially rigid active site,[1] for many other enzymes, binding of substrates or inhibitors induces significant conformational changes. In some cases, the relevant motion is a hinge-bending, which leads to large-scale rigid body displacement of entire domains. Examples of substrate-induced domain motion include elastase and other related proteases,[2] maltodextrin binding protein,[3] a number of kinases including hexokinase and 3-phosphoglycerate kinase,[4–6] and lysozyme.[7,8] In other cases, such as triose phosphate isomerase, the relevant motion is confined to a single loop.[9] In both cases it is of interest to understand the energetics and timescales of such motions. Since the pioneering work by McCammon and Karplus on hen egg lysozyme,[10] a number of theoretical studies have addressed the issues of hinge bending and substrate-induced conformational changes. The proteins whose hinge-bending motions have been studied include L-arabinose binding protein,[11] liver alcohol dehydrogenase,[12] and T4 lysozyme.[13] Recent studies on triose phosphate isomerase have addressed the issues of timescale and energetics for the case of a more localized substrate-induced conformational change.[9,14]

Recently, the first crystal structure for a class II cytochrome P450 was reported.[15] Cytochrome P450BM-3 from *Bacillus megaterium* catalyzes the hydroxylation of fatty acids.[16] Its preferred substrates are 14- to 20-carbon saturated and unsaturated fatty acids. Unlike most class I and class II cytochromes P450, P450BM-3 is catalytically self-sufficient. The holoenzyme contains both an N-terminal heme domain and a C-terminal reductase domain. Genes for the heme domain and the reductase domain have been separately expressed, and the reconstituted system has been shown to be catalytically active.[17,18] The 471 amino acid heme domain has been crystallized and a 2.0 Å resolution structure reported. Interestingly, the asymmetric unit cell contains two enzyme molecules which differ in their conformation around the substrate binding pocket. Molecule 2 in the asymmetric unit has a more open and accessible substrate binding pocket than molecule 1. The difference in conformation is described as rigid body rotations of the N-terminal domain and the FG domain relative to the main

© 1995 WILEY-LISS, INC. *This article is a US Government work and, as such, is in the public domain in the United States of America.

Received May 24, 1994; revision accepted November 14, 1994.

Address reprint requests to Rick L. Ornstein, Environmental Molecular Sciences Laboratory, Pacific Northwest Laboratory, Richland, WA 99352.

body of the enzyme. In this sense the crystal structure of P450BM-3 is reminiscent of the recently reported structures of the M6I mutant of T4 lysozyme which had five different allomorphs in the crystal related to each other by rigid body displacements of the N- and C-terminal domains.[8] Both the more open conformation of molecule 2 of the P450BM-3 crystal and the more closed active site of molecule 1 appear to be stabilized by a number of crystal contacts. Thus, it is unclear whether the two conformations reported by the crystallographers would be highly populated in a noncrystalline environment. In the absence of these crystal contacts, this functionally important region of P450BM-3 could possibly adopt still other conformations than the ones observed in the crystal structure.

We report separate 200 ps molecular dynamics trajectories for each of the molecules in the asymmetric unit of the crystal structure of P450BM-3. Significant rearrangement of the mouth of the substrate binding pocket in molecule 2 occurs upon the removal of the crystal contacts, but such rearrangements are not observed for molecule 1. However, the rearrangement in molecule 2 does not result in it resembling molecule 1. The time-average structures of molecule 1 and molecule 2 are diverging from each other rather than converging to a common structure.

METHODS

The systems for which trajectories were calculated were based on the crystallographically determined structure of P450BM-3.[15] The reported crystal structure was refined to an R factor of 16.9 at 2.0 Å resolution and contained two molecules in the asymmetric unit. Separate trajectories were calculated for each molecule in the asymmetric unit. The modeled system included residues 1–457 of cytochrome P450BM-3, the heme moiety at the active site, crystallographically determined solvent molecules (228 water molecules for molecule 1 and 235 for molecule 2), added sodium and chloride ions, and a 10 Å layer of explicit solvent. The simulations were done using an all-hydrogen model. The initial hydrogen coordinates were generated according to idealized bond lengths and angles using InsightII (Biosym Technologies v2.2). Side chain polar hydrogens were positioned so as to maximize intramolecular hydrogen bonding, using a previously described automated method, NETWORK.[19] Acidic and basic side chains (Asp, Glu, Arg, and Lys), as well as the N- and C-termini, were fully charged. Based on observed hydrogen bonding patterns, all 13 histidine residues were modeled in the unionized state. In order to position the added sodium and chloride ions, the electrostatic potential due to the protein at each added solvent molecule was calculated using the Delphi program (Biosym Technologies v2.4)[20–22] as implemented in InsightII. Since the protein, as modeled, carries a net charge of −16, a compensating number of solvent molecules with large negative electrostatic potentials were first replaced with sodium ions. Then an additional six sodium ions and six chloride ions were added to approximate physiological salt concentrations.

For each simulation, the system was first minimized for 500 steps with all heavy atoms fixed to relax the added hydrogens. Then the solvent molecules and ions were minimized for 500 steps with the protein heavy atoms fixed. This was followed by 5 ps of dynamics on the solvent and ions, followed by a second round of minimization. Finally, 1000 steps of minimization were performed with all atoms free to move allowing any remaining hot spots to relax. The atomic velocities were initialized using a Maxwellian distribution at 50 K, and the system was gradually warmed to 300 K over a period of 10 ps. After this, the simulations were continued at 300 K for 190 ps using a 1.0 fs timestep. The Discover simulation package (Biosym Technologies v2.9) with the consistent valence forcefield of Hagler and coworkers was used in all calculations.[23,24] A constant temperature was maintained by weakly coupling the system to a thermal bath using the method of Berendsen et al.[25] A group-based twin cutoff protocol was used for nonbonded interactions. Interactions between groups closer than 12 Å were calculated every timestep. Interactions between 12 and 15 Å were updated every 20 timesteps. (The use of a longer cutoff has been found to improve the coupling between the solute and solvent temperatures.[26,27]) At the cutoffs, nonbonded interactions were truncated without using a switching function. The default switching function in the Discover simulation package has been shown to give rise to artifacts in trajectories of charged systems.[26]

RESULTS AND DISCUSSION

Before discussing the results of the trajectories, a brief discussion of the structure of the hemoprotein domain of P450BM-3 is in order.[15] The protein is 471 residues in length, of which 1–457 were resolved in the crystallographic structures. The enzyme is a triangular prism consisting of 15 α-helices and 4 β-sheets, which are divided into an α-rich domain and a β-rich domain. The heme cofactor is sandwiched between helices I and L. The substrate binding pocket of cytochrome P450BM-3 is lined by residues from the B′ and F helices and β sheets 1 and 4, including residues Phe-42, Arg-47, Tyr-51, Phe-87, Leu-181, Met-185, Leu-188, Ala-191, Ala-328, Ala-330, Met-354, and Leu-437. The crystal structure contains two molecules per asymmetric unit. Molecule 2 has a more open structure in the vicinity of the substrate binding pocket and differs from molecule 1 by a rotation of the β domain by ~5.0 degrees and helices F and G by ~4.6 degrees, relative to the remainder of the protein. The more open conformation of molecule 2 appears to be sta-

TABLE I. B-Factors of Residues Lining the Substrate Binding Pocket

Residue	Molecule 1 MD (Å^2)	Molecule 1 X-ray (Å^2)	Molecule 2 MD (Å^2)	Molecule 2 X-ray (Å^2)
Phe-42	13.56	36.67	19.53	20.91
Arg-47	27.97	72.08	77.00	66.06
Tyr-51	10.35	17.23	10.04	14.64
Phe-87	10.71	13.45	10.61	16.90
Leu-181	10.49	26.41	28.86	29.56
Met-185	15.29	47.46	64.93	40.07
Leu-188	26.68	49.05	81.84	51.33
Ala-191	39.03	81.37	132.34	82.46
Ala-328	12.05	12.71	11.26	11.67
Ala-330	15.68	16.75	18.52	15.21
Met-354	13.20	20.73	17.06	20.19
Leu-437	20.10	27.60	48.87	24.12
Hem-472	7.23	8.63	8.15	15.26

TABLE II. Calculated Backbone Dihedral Angle Fluctuations for Residues Lining the Substrate Binding Pocket

Residue	Molecule 1 ϕ	Molecule 1 ψ	Molecule 2 ϕ	Molecule 2 ψ
Phe-42	18.74	10.75	13.46	12.27
Arg-47	36.21	16.48	22.13	19.54
Tyr-51	10.46	11.37	12.07	11.28
Phe-87	11.01	9.02	11.35	10.33
Leu-181	9.52	9.75	9.88	9.84
Met-185	10.30	11.05	10.98	9.44
Leu-188	10.68	12.06	12.14	13.11
Ala-191	13.33	14.58	13.76	43.83
Ala-328	11.25	16.67	11.02	8.82
Ala-330	11.28	17.36	11.74	18.40
Met-354	17.50	13.18	20.60	11.60
Leu-437	12.69	11.95	20.68	13.28

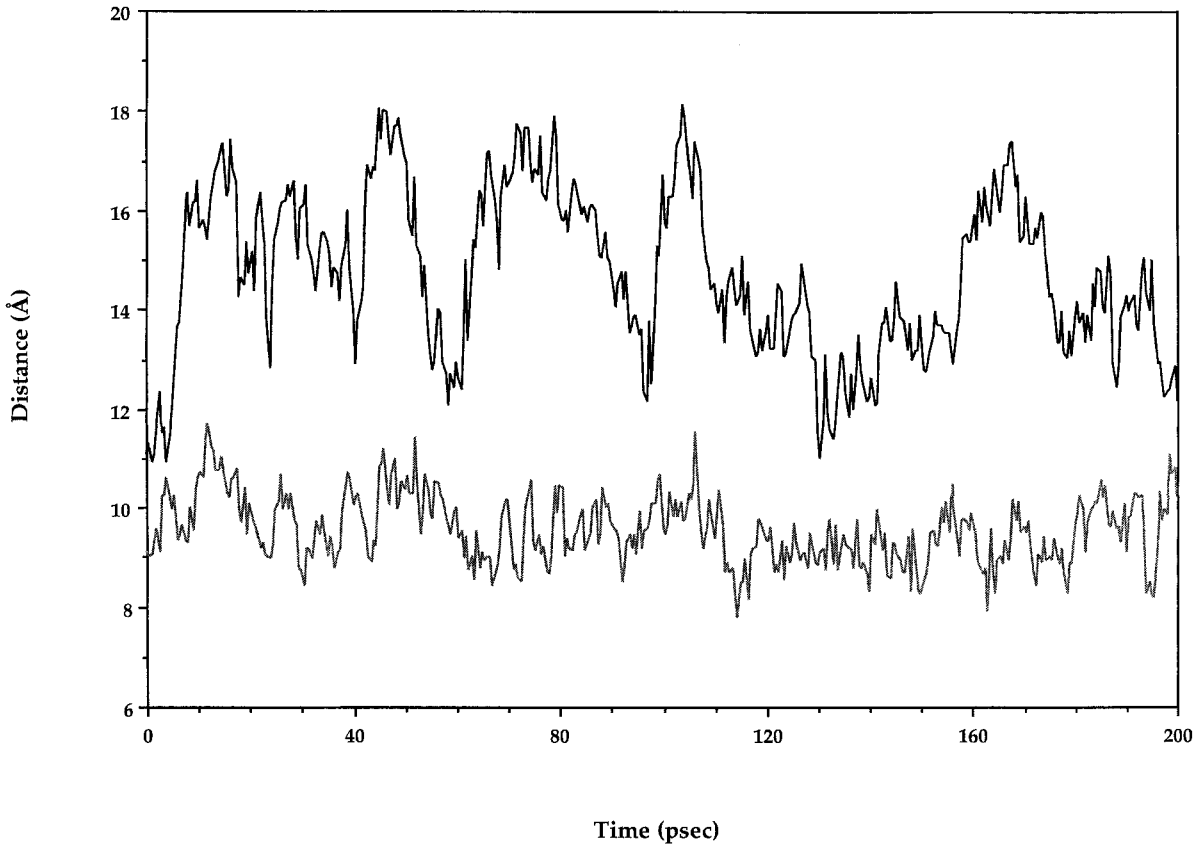

Fig. 1. The distance between the C-alpha carbons of residues 45 and 191 is plotted as a function of the time course of the simulations for molecule 1 (gray) and molecule 2 (black).

bilized by a number of crystal contacts in the N-terminal domain, while the more closed conformation of molecule 1 may be stabilized by a number of crystal contacts in the FG region.

The overall behavior of molecule 1 and molecule 2 was similar in the trajectories. Over the final 150 ps, the average rms deviation in main chain atom coordinates with respect to their crystal structures was 1.19 Å for molecule 1 and 1.53 Å for molecule 2. The higher deviation seen for molecule 2 is due to con-

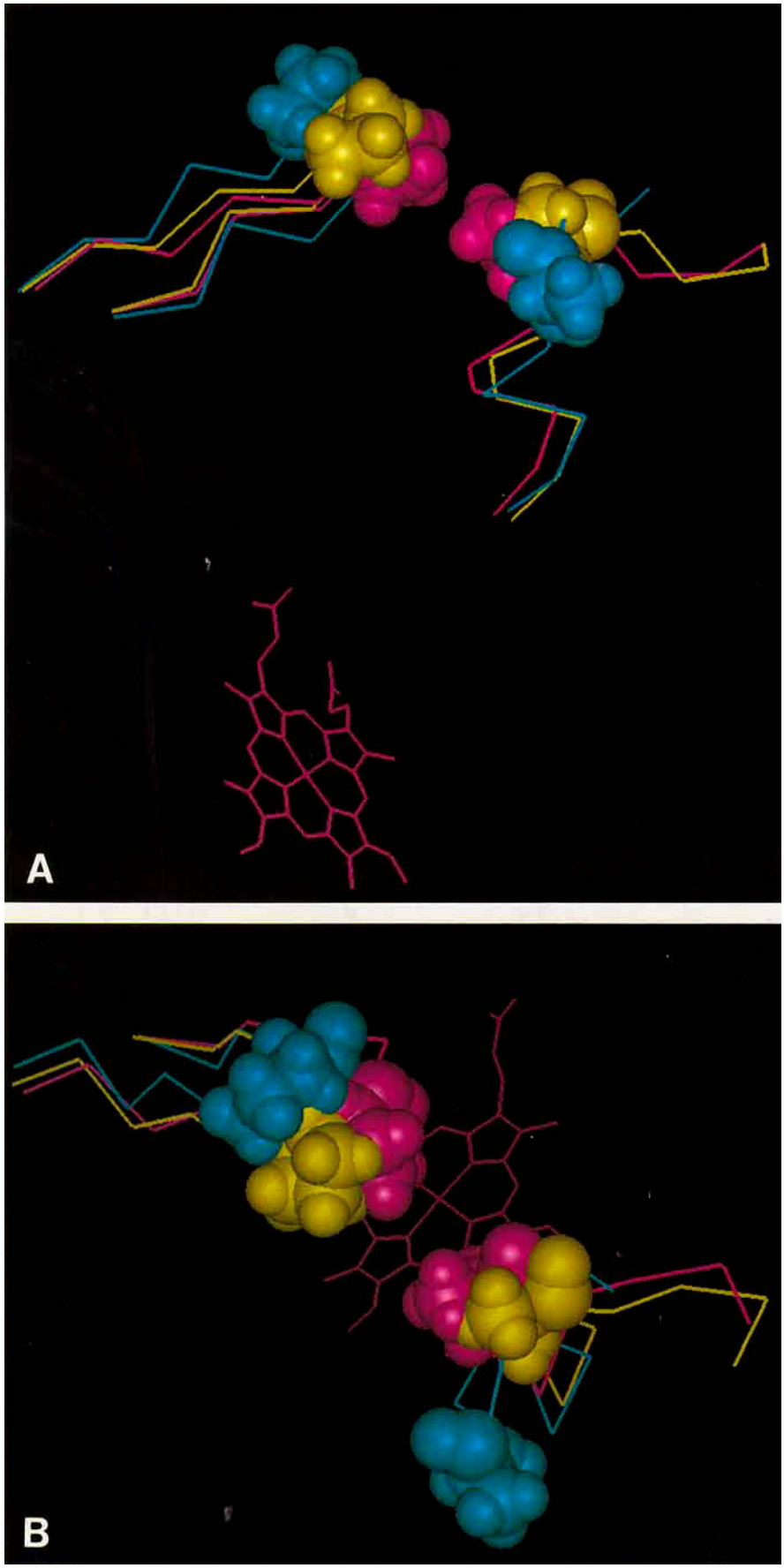

Fig. 2.

formational changes in helices B', G, and I, all of which contribute residues to the substrate binding pocket or access channel. The calculated radius of gyration over the same time period was 22.75 ± 0.07 Å for molecule 1 and 22.87 ± 0.05 Å for molecule 2. The slight increase between molecules 1 and 2 is consistent with the trend seen in the crystal structures. The calculated solvent accessible surface area from the trajectory of molecule 2 (21,825 ± 183 Å^2) is also slightly larger than that of molecule 1 (21,082 ± 175 Å^2), again consistent with the differences seen in the crystal structures and due mostly to the more open nature of the active site pocket in molecule 2 (calculated using the ACCESS program developed by Lee and Richards[28]).

Since the two crystal structures differ most in the substrate binding pocket and access channel, a major question to be answered in analyzing the trajectories was the extent to which the conformation of the two molecules in this region converged when they were simulated as isolated molecules. The rms deviations in main chain atom position between the time-averaged structures of molecule 1 and molecule 2 are larger than between either time-average structure and its corresponding crystal structure. On the time-scale simulated, there is no evidence that the two crystal forms are converging toward a common conformation, which might be more representative of the solution structure.

For the set of 11 active-site residues listed above, the solvent accessible surface area in the crystal structure of molecule 2 is 57% larger than in molecule 1. For both molecules, the accessible area of these active site residues increases during the early portion of the simulation as did the accessible areas of the entire protein. However, the increases in the accessible area of the substrate binding region are larger than the increases observed for the time-average structures of each whole protein. The solvent accessible surface area of these active site residues in the time average structure of molecule 1 increased 22% over the starting structure, while for molecule 2 the increase was 25%. Thus throughout the trajectories, as in the crystal structures, molecule 2 has a more open substrate binding pocket. Again indicating that the simulated structures are not converging.

Calculated and experimental *B*-factors for the residues lining the putative substrate binding pocket are listed in Table I. In these substrate-free trajectories, the residues lining the substrate binding pocket include both very quiet residues and extremely mobile residues. For the molecule as a whole, the calculated fluctuations for molecule 1 (average per residue *B*-factor 24.2 Å^2) are similar to those for molecule 2 (26.8 Å^2). In the substrate binding pocket, there are a few notable exceptions to the trend of similar calculated *B*-factors in the two simulations. Arg-47 is significantly quieter in the simulation of molecule 1 than in the simulation of molecule 2 and several residues in the FG loop of molecule 2 (Met-185, Leu-188, Ala-191) had much larger calculated *B*-factors than in the simulation of molecule 1. For both molecules 1 and 2, for the protein as a whole, there is qualitative agreement between the patterns of large and small calculated *B*-factors and the experimentally determined values (data not shown). However, for molecule 1 the magnitudes of the calculated *B*-factors in the binding pocket are consistently smaller than the experimental values. In particular, Arg-47, Met-185, Leu-188, and Ala-191 have calculated *B*-factors that are only half of the corresponding experimental values. Even though the conformation of the FG loop in the crystal structure of molecule 1 appears to be stabilized by a number of crystal contacts, the experimental *B*-factors are suggestive of high mobility in this region. However, the calculated *B*-factors indicate that this region of molecule 1 is exploring very little conformational space during the trajectory, even though one might expect that the absence of the crystal contacts should enhance mobility in this region. For molecule 2, the calculated *B*-factors for the substrate binding pocket are much more comparable to the experimental values. The particularly large calculated *B*-factors in the FG (Met-185, Leu-188, Ala-191) region indicate that the access channel and substrate binding pocket are exploring a number of different conformations.

The fluctuations in backbone dihedral angles for these active site residues were also determined and are shown in Table II. For both molecules 1 and 2, they are generally small and indicate that, with the exception of Arg-47 in the simulation of molecule 1 and Ala-191 in molecule 2, these active site residues do not undergo any backbone dihedral angle transitions during the trajectories. For comparison, the mean fluctuation in ϕ and ψ for all α-helical residues is 11°, while for residues in β sheets it is 15°. For all other residues, the mean backbone dihedral angle fluctuation is 17°. Interestingly, although residues Leu-181, Met-185, and Leu-188 have large calculated *B*-factors, they do not have large fluctuations in their backbone dihedral angles. These residues are undergoing large displacements due to upstream and downstream backbone dihedral angle transitions rather than to conformational switches in the residues themselves.

Fig. 2. Superimposed C-alpha traces of the FG loop and β sheet 1 in P450BM-3. Residues 45 and 191 at the mouth of the active site pocket are shown in spacefilling representation. Also shown is the heme cofactor at the bottom of the substrate binding pocket. The trace in magenta is from the X-ray structure of molecule 1. The trace in yellow is from the X-ray structure of molecule 2 while the trace in cyan is from the structure at 104 psec in the molecular dynamics trajectory of molecule 2. The structures were superimposed on the main chain atoms of α-helices C, D, E, H, I, J, K, and L.

The contrast between the flexibility of molecule 2 and the stability of molecule 1 can be clearly seen by examining the mouth of the substrate binding pocket. Figure 1 shows the time course of the distance between the C-alpha atoms of residues 45 and 191 for molecules 1 and 2. These residues, the first in the loop between the F and G helices and the second in the turn between two strands of β sheet 1, define part of the mouth of the substrate binding pocket. In the energy minimized structure of molecule 1, this distance is 9.1 Å versus 11.1 Å in molecule 2, reflecting the fact that molecule 2 has a more open structure. For molecule 1, this distance does not change significantly during the trajectory, nor does it undergo significant fluctuations. Its average value is 9.5 ± 0.6 Å. On the other hand, the mouth of the substrate binding pocket widens significantly in molecule 2 to an average value of 14.7 Å with much larger fluctuations of 1.6 Å. During the trajectory, the mouth of the active site of molecule 2 widens and narrows repeatedly, ranging from 10.9 to 18.1 Å. It is this motion which gives rise to the large calculated *B*-factors for residues 181, 185, 188, and 191 noted above. In a couple of instances, molecule 1 does explore conformations where the distance between residues 45 and 191 has increased to more than 11 Å, the value seen in the crystal structure of molecule 2. However, a closer examination of these outlying conformations of molecule 1 indicates that they are still much more reminiscent of the molecule 1 crystal and time-averaged structures than they are of the crystal and time-averaged structures of molecule 2. In addition although molecule 2 explores a number of conformations in this region, never during the simulation is a conformation sampled in which the mouth of the active site closed down to resemble molecule 1. Two views of the substrate binding pocket and docking region are shown in Figure 2. The superimposed C-alpha traces are from the crystal structures of molecule 1 and molecule 2 and from the trajectory of molecule 2 at 104 ps, when the distance between residues 45 and 191 reaches its maximum value. The C-terminal residues of helix F, the N-terminal residues of helix G, the residues in the FG loop, and residues in β sheet 1 are all moving as part of the opening and closing motion of the mouth of the substrate binding pocket.

Although the differences between the crystal structures of molecule 1 and molecule 2 are quite small compared for instance to the differences seen between the five allomorphs in the crystal structure of the M6I mutant of T4 lysozyme, the timescale for convergence of the two structures appears to be much longer than in the case of T4 lysozyme. In a recent series of MD simulations of the M6I mutant of T4 lysozyme, the most open and most closed allomorphs of T4 lysozyme showed clear indications of converging on a common structure during the early portions of 500 ps simulations (Arnold and Ornstein, submitted). In summary, the present P450BM-3 simulations indicate that the mouth of the substrate binding pocket is highly mobile, and this may influence the ability of the enzyme to accommodate substrates of varying size. However, since the opening and closing occurs on such a rapid timescale (tens of ps) relative to substrate binding, the gating motion is not expected to significantly modulate the rate of substrate binding. Since the substrate binding pocket is so dynamic, it is likely that the range of substrates which could bind is broader than would be deduced from an examination of just the crystal structure. In addition, the dynamic nature of the mouth of the active site complicates any attempt to identify key residues crucial for substrate binding.

ACKNOWLEDGMENTS

We thank Professors Julian A. Peterson and Johann Deisenhofer of the University of Texas Southwestern Medical Center at Dallas for supplying the P450BM-3 coordinates and Professor Peterson for comments on the manuscript. This work was supported by grant KP0402 from the Health Effects and Life Sciences Research Division of the Office of Health and Environmental Research of the Office of Energy Research of the U.S. Department of Energy (RLO). Pacific Northwest Laboratory is a multiprogram national laboratory operated for the U. S. Department of Energy by Battelle Memorial Institute under contract DE-AC06-76RLO 1830.

REFERENCES

1. Poulos, T.L., Raag, R. P450cam: Crystallography, oxygen activation, and electron transfer. FASEB J. 6:674–679, 1992.
2. Holland, D.R., Tronrud, D.E., Pley, H.W., Flaherty, K.M., Stark, W., Jansonius, J.N., McKay, D.B. Matthews, B.W. Structural comparison suggests that thermolysin and related neutral proteases undergo hinge-bending motion during catalysis. Biochemistry 31:11310–11316, 1992.
3. Sharff, A.J., Rodseth, L.E., Spurlino, J.C., Quiocho, F.A. Crystallographic evidense of a large ligand-induced hinge-twist motion between the two domains of the maltodextrin binding protein involved in active transport and chemotaxis. Biochemistry 31:10657–10663, 1992.
4. Olsen, L.R., Reed, G.H. The structure of the manganese(II)-ADP-nitrate-lyxose complex at the active site of hexokinase. Arch. Biochem. Biophys. 304:242–247, 1993.
5. Adams, B., Pain, R.H. The effect of substrates on the interdomain interactions of the hinge-bending enzyme 3-phophoglycerate kinase. FEBS Lett. 196:361–364, 1986.
6. Gerstein, M., Schulz, G., Chothia, C. Domain closure in adenylate kinase. Joints on either side of two helixes close like neighboring fingers. J. Mol. Biol. 229:494–501, 1993.
7. Dixon, M.M., Nicholson, H., Shewchuk, L., Baase, W.A., Matthews, B.W. Structure of a hinge-bending bacteriophage T4 lysozyme mutant, Ile3 → Pro. J. Mol. Biol. 227: 917–933, 1992.
8. Faber, H.R., Mathews, B.W. A mutant T4 lysozyme displays five different crystal conformations. Nature (London) 348:263–266, 1990.
9. Joseph, D., Petsko, G.A., Karplus, M. Anatomy of a conformational change: hinged "lid" motion of the triosephosphate isomerase loop. Science 249:1425–1428, 1990.
10. McCammon, J.A., Gelin, B.R., Karplus, M., Wolynes, P.G. The hinge-bending mode in lysozyme. Nature (London) 262:325–326, 1976.

11. Mao, B., McCammon, J.A. Structural study of hinge-bending in L-arabinose-binding protein. J. Biol. Chem. 259: 4964–4970, 1984.
12. Colonna-Cesari, F., Perahia, D., Karplus, M., Eklund, H., Branden, C.I. Tapia, O. Interdomain motion in liver alcohol dehydrogenase: Structural and energetic analysis of the hinge bending mode. J. Biol. Chem. 261:15273–15278, 1986.
13. Arnold, G.E., Manchester, J.I., Townsend, B.D., Ornstein, R.L., Investigations of domain motions in bacteriophage T4 lysozyme J. Bio. Mol. Struc. Dyn. 12:457–474, 1994.
14. Wade, R.C., Davis, M.E., Luty, B.A., Madura, J.D., McCammon, J.A. Gating of the active site of triose phosphate isomerase: Brownian dynamics simulations of flexible peptide loops in the enzyme. Biophys. J. 64:9–15, 1993.
15. Ravichandran, K. G., Boddupalli, S. S., Hasemann, C. A., Peterson, J. A., Deisenhofer, J. Crystal structure of hemoprotein domain of P450BM-3, a prototype for microsomal P450's. Science 261:731–736, 1993.
16. Fulco, A. J. P450BM-3 and other inducible bacterial P450 cytochromes: Biochemistry and regulation. Annu. Rev. Pharmacol. Toxicol. 31:177–203, 1991.
17. Oster, T., Boddupalli, S. S., Peterson, J. A. Expression, purification, and properties of the flavoprotein domain of cytochrome P450BM-3. J. Biol. Chem. 266:22718–22725, 1991.
18. Boddupalli, S. S., Oster, T., Estabrook, R. W., Peterson, J. A. Reconstitution of the fatty acid hydroxylation function of cytochrome P450BM-3 utilizing its individual recombinant hemo- and flavoprotein domains. J. Biol. Chem. 267: 10375–10380, 1992.
19. Bass, M. B., Hopkins, D. F., Jaquysh, W. A. N., Ornstein, R. L. A method for determining the positions of polar hydrogens added to a protein structure that maximizes protein hydrogen bonding. Proteins 12:266–277, 1992.
20. Klapper, I., Hagstrom, R., Fine, R., Sharp, K., Honig, B. Focusing of electric fields in the active site of copper-zinc superoxide dismutase: effects of ionic strength and amino acid modification. Proteins 1:47–59, 1986.
21. Gilson, M., Honig, B. Calculation of electrostatic potentials in an enzyme active site. Nature (London) 330:84–86, 1987.
22. Sharp, K., Honig, B. Electrostatic interactions in macromolecules: theory and applications. Annu. Rev. Biophys. Chem. 19:310–322, 1990.
23. Hagler, A. T. Theoretical simulations of conformation, energetics, and dynamics of peptides. In: "The Peptides." Hruby, V. J., Meienhofer, J. (eds.). New York: Academic Press, 1985: Vol. 7, 213–299.
24. Dauber-Osguthorpe, P., Roberts, V. A., Osguthorpe, D. J., Wolff, J., Genest, M., Hagler, A. T. Structure and energetics of ligand binding to proteins: *Escherichia coli* dihydrofolate reductase-trimethoprim, a drug-receptor system. Proteins 4:31–47, 1988.
25. Berendsen, H. J. C., Postma, J. P. M., van Gunsteren, W. F., DiNola, A., Haak, J. R. Molecular dynamics with coupling to an external bath. J. Chem. Phys. 81:3684–3690, 1984.
26. Arnold, G. E., Ornstein, R. L. An evaluation of implicit and explicit solvent model systems for the molecular dynamics simulations of bacteriophage T4 lysozyme. Proteins 18:19–33, 1994.
27. Guenot, J., Kollman, P. A. Conformational and energetic effects of truncating nonbonded interactions in an aqueous protein dynamics simulation. Prot. Sci. 1:1185–1205, 1992.
28. Lee, B., Richards, F. M. The interpretation of protein structures: Estimation of static accessibility. J. Mol. Biol. 55:379–400, 1971.